Gruppetta, S., Lacombe, F. & Puget, P. (2005). Study of the dynamic aberrations of the human tear film. Optical Express, 13(19), pp. 7631-7636. doi: 10.1364/OPEX.13.007631

Study of the dynamic aberrations of the human tear film

Steve Gruppetta, François Lacombe and Pascal Puget

Laboratoire d'Etudes Spatiales et d'Instrumentation en Astrophysique, Observatoire de Paris, 5, place Jules Janssen, 92195 Meudon, France

steve.gruppetta@obspm.fr

Abstract: The dynamic aberrations introduced by the human tear film are studied by measuring the topography of the tear film surface on 14 subjects using a curvature sensing setup. The RMS wavefront error variation of the data obtained is presented showing the non-negligible contribution of the tear film to overall eye aberrations. The tear film wavefronts are decomposed in their constituent Zernike terms, showing stronger contributions from 4th order terms and terms with vertical symmetry, and the temporal behaviour of these aberrations is analysed.

OCIS codes: (170.4460) Ophthalmic optics; (330.5370) Physiological optics; (010.7350) Wave-front sensing and (010.1080) Adaptive optics.

References and links

1. J. Liang, D. R. Williams, and D. T. Miller, "Supernormal vision and high-resolution retinal imaging through adaptive optics," J. Opt. Soc. Am. A **14,** 2884–2892 (1997).
2. M. Glanc, E. Gendron, F. Lacombe, D. Lafaille, J.-F. L. Gargasson, and P. Léna, "Towards wide-field retinal imaging with adaptive optics," Opt. Commun. **230,** 225–238 (2004).
3. E. J. Fernández, I. Iglesias, and P. Artal, "Closed-loop adaptive optics in the human eye," Opt. Lett. **26,** 746–748 (2001).
4. A. Roorda, F. Romero-Borja, W. J. Donnelly III, H. Queener, T. J. Hebert, and M. C. Campbell, "Adaptive optics scanning laser ophthalmoscopy," Opt. Express **10,** 405–412 (2002), http://www.opticsexpress.org/abstract.cfm?URI=OPEX-10-9-405
5. L. Diaz-Santana, C. Torti, I. Munro, P. Gasson, and C. Dainty, "Benefit of higher closed-loop bandwidths in ocular adaptive optics," Opt. Express **11,** 2597–2605 (2003), http://www.opticsexpress.org/abstract.cfm?URI=OPEX-11-20-2597
6. H. Hofer, P. Artal, B. Singer, J. L. Aragón, and D. R. Williams, "Dynamics of the eye's wave aberration," J. Opt. Soc. Am. A **18,** 497–505 (2001).
7. K. M. Hampson, I. Munro, C. Paterson, and C. Dainty, "Weak correlation between the aberration dynamics of the human eye and the cardiopulmonary system," J. Opt. Soc. Am. A **22,** 1241–1250 (2005).
8. J. I. Prydal, P. Artal, H. Woon, and F. Campbell, "Study of human precorneal tear film thickness and structure using laser interferometry," Invest. Ophth. Vis. Sci. **33,** 2006–2011 (1992).
9. T. J. Licznerski, H. T. Kasprzak, and W. Kowalik, "Analysis of shearing interferograms of tear film by the use of fast Fourier transforms," J. Biomed. Opt. **3,** 32–37 (1998).
10. R. Tutt, A. Bradley, C. Begley, and L. N. Thibos, "Optical and visual impact of tear break-up in human eyes," Invest. Ophth. Vis. Sci. **41,** 4117–4123 (2000).
11. A. Dubra, C. Paterson, and C. Dainty, "Study of the tear topography dynamics using a lateral shearing interferometer," Opt. Express **12,** 6278–6288 (2004), http://www.opticsexpress.org/abstract.cfm?URI=OPEX-12-25-6278
12. R. Montés-Micó, J. L. Alió, G. Muñoz, J. J. Pérez-Santoja, and W. N. Charman, "Postblink changes in total and corneal ocular aberrations," Ophthalmology **111,** 758–767 (2004).
13. K. Y. Li, G. Yoon, and G. Pan, "Variability in retinal image quality with tear film behavior after blink," Invest. Ophth. Vis. Sci. **46**, E–Abstract 848 (2005).
14. S. Gruppetta, L. Koechlin, F. Lacombe, and P. Puget, "A curvature sensor for the measurement of the static corneal topography and the dynamic tear film topography in the human eye," Opt. Lett. **30,** (2005, in press).

#8157 - $15.00 USD Received 18 July 2005; revised 8 September 2005; 13 September 2005

1. Introduction

The study of the human eye's aberrations has a long history, however it is only recently that interest in the dynamic component of these aberrations has arisen. This interest has been strongly linked with adaptive optics making the jump from astronomy to ophthalmology, where these dynamic aberrations are measured and corrected in a closed loop [1, 2, 3, 4, 5]. However, whereas in astronomy the atmospheric aberrations are very well understood, their ocular counterparts are less so. Suggestions have been made that the changes in ocular aberrations could be due to, in varying degrees, eye movements, retinal pulsation, microfluctuations of the lens and variations in the tear film layer [6, 7]. This paper focuses on the latter of these.

The human tear film provides the first and most powerful optical surface in the eye by having a large curvature and the largest refractive index step in the eye's optics. Furthermore, the tear film is a liquid layer, and the effect on this liquid layer of eye movements, pressure exerted by the eye lids, evaporation and other external factors is a non-static air-tear film interface. Consequentially, the aberrations introduced by this layer are also dynamic.

Though considerable work has been done on measuring the average thickness of the tear film layer and the film's break up time [8, 9, 10], much less is known on the actual aberrations introduced and their temporal behaviour. Dubra *et al.* [11] have used lateral shearing interferometry to monitor the effect of the tear film on the optical quality showing small but non-negligible variation in the wavefront error with time, while Montés-Micó *et al.* [12] use a commercial topographer to show a degradation of the optical quality after time intervals of 10s and 20s following a blink. Other work is also currently underway using a Shack-Hartmann sensor [13].

2. Measuring the dynamic tear film aberrations

In the work presented in this paper, a curvature sensor is used to measure the tear film topography. Incoherent light is used to illuminate the cornea and the intensity of the aberrated wavefront reflected from the air-tear film interface is measured using CCD cameras at 2 planes conjugate to defocused corneal planes. The difference of these intensity signals is then used to calculate the topography of the tear film. The technique and optical setup used have been described in detail in reference 14. The advantage of this technique is that it enables fast and continuous acquisition with simple and accurate wavefront reconstruction which allows the monitoring of the dynamic tear film surface. The topography elevation values are multiplied by the difference in refractive indices of air ($n = 1.000$) and the tear film ($n = 1.337$) to give the wavefront transmitted through the tear film. This does not take into account inhomogenieties in the tear film layers (in particular the varying thickness of the lipid layer) which have different refractive indices. All further references to tear film wavefronts in this paper refer to the transmitted wavefronts.

Data was collected for 14 subjects with no tear abnormalities; several series of tear film wavefronts were recorded at 22Hz for each subject. The diameter of the measured pupil was 4mm. Most of the subjects were non-contact lens wearers, and for the 2 soft contact lens wearers data was collected with and without the lens worn. The measuring system being very sensitive to eye movements, data was collected only when the cornea was within a tolerance range of $\pm 150\mu$m from the measuring position in the horizontal and vertical directions ($< 8\%$ of the pupil diameter), and $\pm 300\mu$m in the axial direction. This sensitivity ensures that for the data collected, the positioning of the eye is very accurate and movements are kept to a minimum; the drawback however is that this makes data collection harder since, even using a chin rest and a restrictive head rest, it is not straightforward for subjects to keep their eyes within the required range. The changes in aberrations measured for a calibrating surface when translated across these tolerance ranges was found to be negligible with respect to the measured tear film aberration changes. In addition, typical power spectra of the aberration changes, which are discussed later, do not show particularly strong contributions in the 2-3Hz region which would

#8157 - $15.00 USD Received 18 July 2005; revised 8 September 2005; 13 September 2005

correspond to microsaccadic eye movements.

The series of tear film wavefronts obtained vary in length between 2s and 15s depending on how long the subject was able to keep within the required range for data acquisition. Examples of the data collected are shown in the videos in Fig. 1, which show the evolution of the wavefront for 2 subjects following a blink after removal of first and second order Zernike terms. The acquired images also allowed the observation of the effect of blinking on the tear film immediately before and after the blink, as shown in Fig. 2.

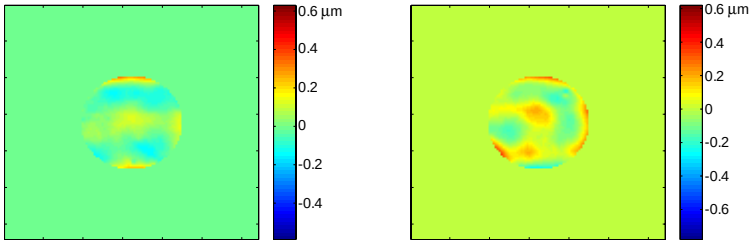

Fig. 1. Videos showing the evolution of the wavefront transmitted through the tear film at 22Hz for subjects 2 (left, 2MB) and 7 (right, 1MB.)

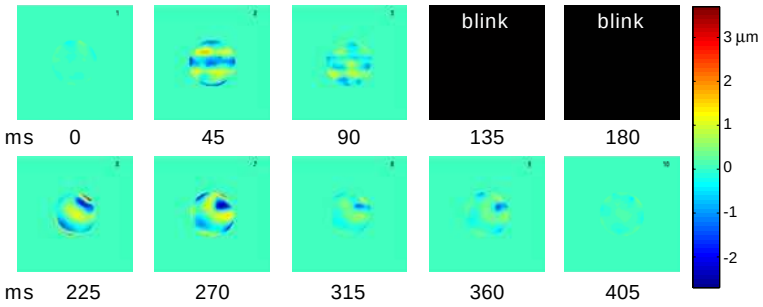

Fig. 2. Series showing 'wrinkles' being formed on the tear film as the eye lids exert pressure on it at the start of the blink, and a brief unstable period after the blink.

3. Results

3.1. Evolution of the tear film wavefront RMS error

Figure 3 shows the typical evolution of the RMS wavefront error after removal of first and second order Zernike terms. The static component of these plots is largely due to corneal aberrations, whereas the dynamic component is due to the tear film dynamics. In Fig. 3(b), the dashed line indicates the break up of the tear film and the RMS wavefront error increases steadily thereafter as the dry patches on the cornea grow. In Fig. 3(c), the evolution of the RMS wavefront error is shown for subject 6 with and without soft contact lenses worn, showing a higher RMS error value and larger variations when the contact lens was worn. The number of contact lens wearers in the group of subjects was however too small to analyse further the effect of contact lenses on the tear film. Average values for the RMS error evolution were calculated over the series of data collected. Figure 4 shows two plots representing the average RMS evolution over all series 2s and 6s in length respectively. These plots show a relatively constant trend due to the large inter-subject variablilty, as shown by the standard deviation on the plots. Longer acquisition times were not possible due to the prolonged accuracy in eye positioning required,

#8157 - $15.00 USD Received 18 July 2005; revised 8 September 2005; 13 September 2005

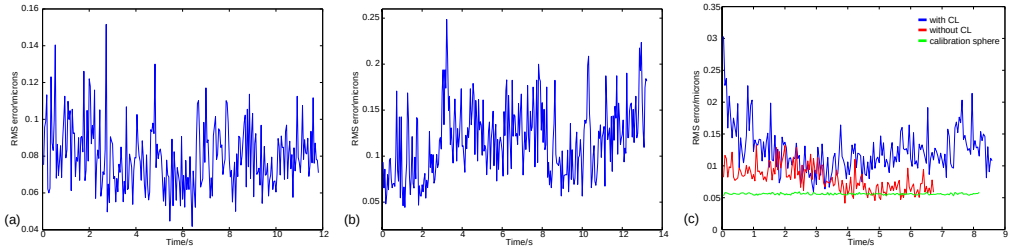

Fig. 3. Typical evolution of the RMS wavefront error. (a) Subject 2. (b) Subject 11. (c) Subject 6 with (blue) and without (red) contact lens. The RMS wavefront error for a static calibration surface is also shown (green.)

and hence trends for longer time intervals are not available. Different trends might also be observed for pupil sizes larger than the largest pupil possible in this study (4mm) as suggested by Montés-Micó *et al.* [12]. Tear film break-up was not measured in this study. A future study combining this setup with measurement of the tear film break-up would give further knowledge on the effect of break-up on the tear film topography.

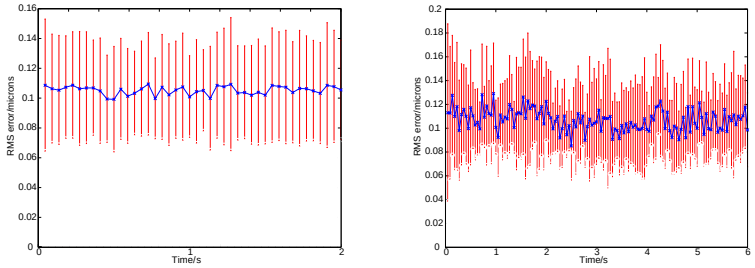

Fig. 4. Average evolution of the RMS wavefront error over all 2s series following a blink (left, 42 series from 14 subjects) and 6s series following a blink (right, 13 series from 11 subjects) and their standard deviation.

3.2. Zernike polynomial decomposition of the series of wavefronts

To obtain a better insight into the varying tear film aberrations, the series of wavefronts obtained were decomposed into Zernike polynomials. Figure 5 shows the evolution of Zernike terms for orders 3 to 6 for the series for subject 11 represented in Fig. 3(b). The figure shows that the strongest contributions are due to the lower orders, particularly the 4th order terms. This can also be seen from the histograms in Fig. 6 representing the Zernike coefficients averaged over all frames of all 2s and 6s series; the average 4th order coefficient is 2.9 times larger than the average 5th order coefficient for the 6s series.

The histograms in Fig. 6 also indicate differences between the positive and negative azimuth orders showing higher contributions to the wavefront aberrations of the positive azimuth orders which represent aberrations with vertical symmetry. This can be seen, for example, with the coefficient representing fourth order coma at 0°, ${Z^2}_4$ which for the 6s series is 84% larger than its counterpart at 45°, ${Z^{-2}}_4$, and similarly with tetrafoil at 0° and at 45°, ${Z^4}_4$ and ${Z^{-4}}_4$ respectively, with the former being 48% larger. This asymmetry can be attributed to the pressure exerted in the vertical direction by the upper and lower eyelids on the tear film contributing to larger components in this direction.

#8157 - $15.00 USD Received 18 July 2005; revised 8 September 2005; 13 September 2005

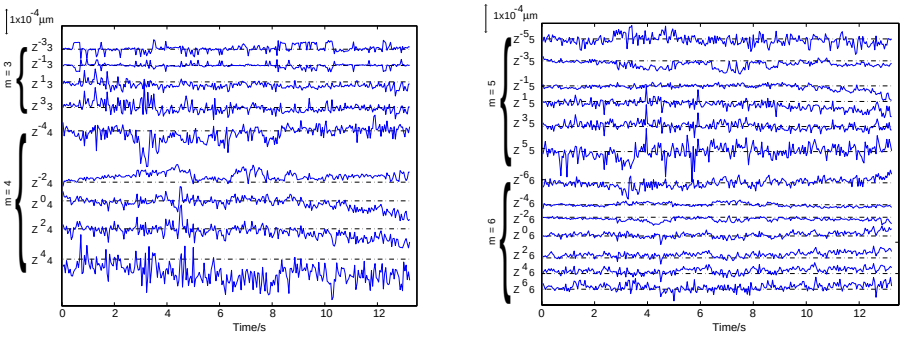

Fig. 5. Typical evolution of Zernike terms for the 3rd and 4th orders (left) and the 5th and 6th orders (right) for subject 11.

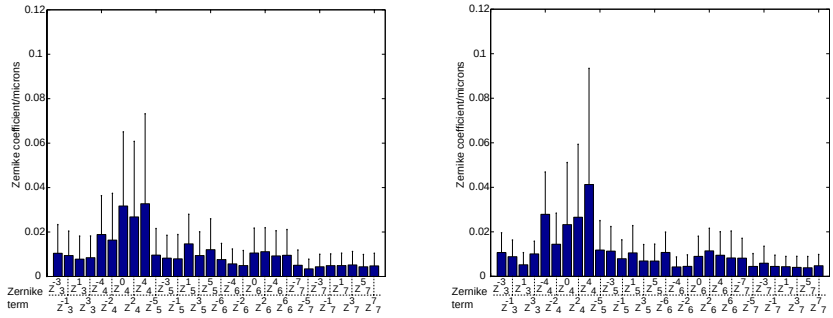

Fig. 6. Magnitudes of the Zernike coefficients averaged over all 2s long series (left) and 6s long series (right) collected, with the average of the standard deviations representing variations within each series.

The wavefronts measured were also compared with wavefronts reconstructed using different numbers of Zernike orders. The RMS difference between the original and reconstructed wavefronts are shown in Fig. 7(a) showing good convergence after the first few orders. Nevertheless, we can see that certain tear film features are not well represented even by reconstructed wavefronts upto the 9th Zernike order, as shown in Fig. 7(b) and (c) which represent respectively a measured wavefront and the reconstructed wavefront. For example, the small blue patch towards the upper left of the pupil in the original is absent in the reconstructed wavefront.

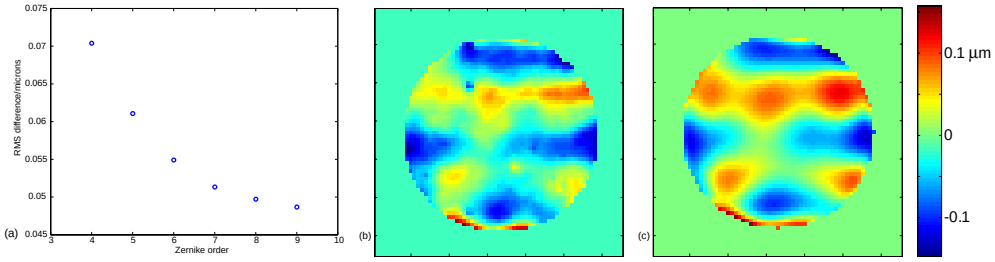

Fig. 7. (a) The RMS difference between the original wavefront and wavefronts reconstructed using different number of Zernike orders. (b) A measured wavefront and (c) the same wavefront reconstructed using Zernike terms upto the 9th order.

#8157 - $15.00 USD Received 18 July 2005; revised 8 September 2005; 13 September 2005

3.3. *Frequency domain analysis*

In order to look at the temporal frequency contributions of the tear film aberrations, the power spectra of the RMS wavefront error plots shown in section 3.1 were computed. A typical power spectrum obtained is shown in Fig. 8. From the linear axis plot we can observe that the strongest contributions to the tear film aberration changes are due to the lower frequencies, typically lower than 2Hz. Such changes are within the scope of most adaptive optics systems which run at closed loop bandwidths of the order of 2-5Hz [1, 2, 3, 4]. However, the comparison of the power spectrum with the noise threshold of the system (determined by calculating the power spectrum obtained from a static surface), as shown in the logarithmic axis plot in Fig. 8, shows that there are measurable contributions to the tear film aberrations at least up to 11Hz, which is the highest frequency measurable in this work. The presence of these higher frequency components might corroborate the argument for using higher closed loop bandwidths in adaptive optics systems [5], though the improvement in optical quality this would bring might be small, especially in relation to the higher technical challenges required for running at higher bandwidths. It should be noted that frequencies just below the Nyquist frequency are boosted by aliasing effects due to frequencies just above this frequency. Furthermore, a similarity can be noted between the power spectrum obtained for tear film variations in this work and those obtained elsewhere for overall dynamic eye aberrations [5, 6].

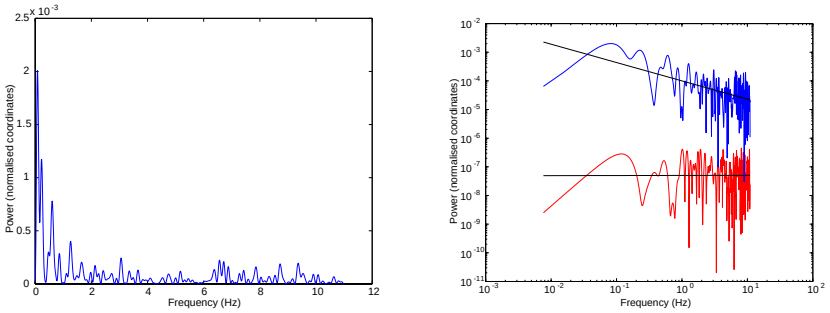

Fig. 8. Power spectrum of the RMS wavefront error variation for subject 11: linear axis plot on the left and a log-log plot on the right together with the power spectrum obtained with a static calibration surface (red.) A least squares error linear fit was applied to these spectra.

4. Conclusion

The wavefronts aberrated by the tear film were measured in this work for a group of healthy eyes. The variation in optical quality due to the tear film indicates that the tear film contributes to the overall optical quality of the eye. It was also discussed that the measurement of tear film break-up would be a useful addition to this work. Stronger contributions to tear film aberrations were observed from 4th order Zernike terms, and in particular from those terms with vertical symmetry. Furthermore, from the temporal point of view, the strongest tear film contributions were observed at low frequencies.

Acknowledgments

The authors would like to thank Laurent Koechlin from the Observatoire Midi Pyrénées for the loan of equipment used in this study, assistance in modifying it and other helpful discussions. Steve Gruppetta is funded by the European Union Research and Training Network SHARP-EYE, contract number HPRN-CT-2002-00301.